

Simulating current diffusion in a stellarator with self-consistent evolution of the equilibrium

F. Solfronk^{*1,2}, E. Fable¹, E. Buglione-Ceresa³, G. Tardini¹, M. Zanini³, S. Kwak³,
H. Zohm^{1,2} and the W7-X Team⁴

¹Max-Planck-Institut für Plasmaphysik, 85748 Garching, Germany

²Ludwig-Maximilians-Universität München, 80539 München, Germany

³Max-Planck-Institut für Plasmaphysik, 17491 Greifswald, Germany

⁴See the author list of O. Grulke *et al* 2026 *Nucl. Fusion* **66** 116003

fabian.solfronk@ipp.mpg.de

Abstract

Accurate prediction of plasma evolution is essential for the development of future tokamak and stellarator reactor scenarios. ASTRA is a 1D integrated transport modelling code originally developed primarily for tokamak applications and therefore partly based on axisymmetric assumptions. Here, we present recent extensions of ASTRA for stellarator applications, including a generalised geometrical description, a generic current diffusion equation formulated in terms of the poloidal magnetic flux, and coupling to the 3D equilibrium code VMEC for self-consistent updates of magnetic-geometry quantities. The upgraded model enables the magnetic equilibrium, bootstrap current, conductivity, and rotational transform to be evolved in stellarator geometry. Validation against Wendelstein 7-X (W7-X) discharge 20171206.036 shows that the experimentally measured toroidal current evolution is reproduced with good accuracy.

1 Introduction

In its original formulation, the 1D integrated transport modelling code ASTRA8 [1, 2] was developed mainly for tokamak applications, and parts of the code relied on axisymmetric assumptions. This has limited its direct application to stellarators. Extending ASTRA to stellarator geometry provides a common transport solver for both tokamaks and stellarators, thereby facilitating comparative studies between the two device concepts. It also represents an important step towards applying the Fenix flight simulator framework [3], which employs ASTRA, to stellarator reactor studies.

For this purpose, ASTRA has been generalised for stellarator geometry through an updated geometrical description and a generic current diffusion equation [4]. Coupling to VMEC [5, 6] and DKES [7] enables the magnetic equilibrium, bootstrap current, conductivity, and rotational transform to evolve self-consistently. In the following, applications of the extended ASTRA framework are presented.

2 Upgrading ASTRA8 for stellarators

A key component of the recent ASTRA extensions is the implementation of a generalised current diffusion equation for the poloidal magnetic flux, Ψ , applicable to both tokamak and stellarator configurations [4]. This equation takes the form

$$\sigma_{\parallel} \left(\frac{\partial \Psi}{\partial t} - \frac{\rho \dot{B}_0}{2B_0} \frac{\partial \Psi}{\partial \rho} \right) = \frac{2\pi B_0 \rho}{\mu_0} (S_{21}\iota + S_{22})^2 \frac{\partial}{\partial \rho} \left[\frac{1}{S_{21}\iota + S_{22}} \left(\frac{S_{11}}{2\pi B_0 \rho} \frac{\partial \Psi}{\partial \rho} + S_{12} \right) \right] - \frac{V'}{2\pi \rho} (j_{BS} + j_{CD}). \quad (1)$$

Here, σ_{\parallel} denotes the parallel electrical conductivity, ρ is the radial coordinate, B_0 is the reference magnetic field, and V' is the radial derivative of the plasma volume. The rotational transform is given by $\iota \equiv \partial \Psi / \partial \Phi$, with Φ denoting the toroidal magnetic flux. The source terms j_{BS} and j_{CD} correspond to the bootstrap current and current drive contributions, respectively. The elements S_{ij} of the susceptance matrix are three-dimensional geometrical factors, as defined in [4]. In the axisymmetric tokamak limit, the off-diagonal elements vanish, whereas in stellarator geometry the terms S_{12} and S_{21} are generally non-zero. Since $\iota \equiv \partial \Psi / \partial \Phi$, the solution of equation (1) also determines the evolution of the rotational transform profile. Furthermore, the total toroidal plasma current can be obtained from [4]

$$I_{\text{tor}} = \frac{S_{11}(\rho_B)}{\mu_0} \left(\frac{\partial \Psi}{\partial \rho} \Big|_{\rho_B} - 2\pi B_0 \rho_B \iota_{\text{vac}}(\rho_B) \right). \quad (2)$$

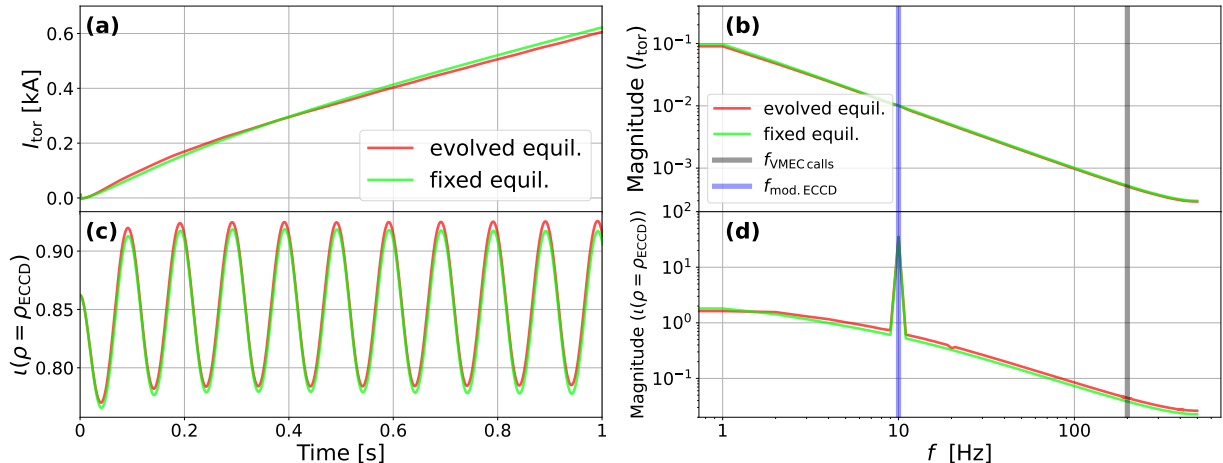


Figure 1: High frequency case: (a)/(b) and (c)/(d): Evolution/Frequency spectrum of I_{tor} and $\iota(\rho = \rho_{\text{ECCD}})$. Comparison between fixed (green) and evolved equilibrium (red). ECCD modulation frequency (blue) and VMEC call frequency (grey) are indicated as vertical lines.

To account for the time-dependent magnetic geometry in a self-consistent manner, ASTRA has been coupled to the three-dimensional equilibrium solver VMEC [6]. This coupling enables the equilibrium to be recomputed during the transport simulation, ensuring that geometry-dependent quantities, including the factors S_{ij} , are updated consistently with the evolving plasma state.

In addition, ASTRA has been linked to DKES through look-up tables [7]. In combination with the evolving VMEC equilibrium, this allows neoclassical transport coefficients and the bootstrap current to be evaluated, and also enables the radial electric field to be advanced consistently. These developments provide the basis for modelling stellarator plasmas in ASTRA with coupled current and equilibrium evolution. Applications of this framework are presented in the following sections.

3 Nonlinear current response

In this section, a proof-of-concept case is considered to investigate the dynamic evolution of the plasma current and rotational transform with self-consistent equilibrium evolution. The electron temperature, density, and effective charge are taken from the W7-X discharge 20171206.036 at ($t=7.8$ s) (see section 4, figure 3), while the bootstrap current is calculated using the DKES coupling described in [7]. Using the ray-tracing code TRAVIS [8], the experimental electron cyclotron current drive (ECCD) is calculated and modulated in our test case according to

$$j_{\text{ECCD}}(t) = \sin\left(\frac{2\pi}{T}t\right) j_{\text{ECCD},t=7.8\text{s}} \quad (3)$$

and simulations are performed for modulation periods of $T_1 = 0.1$ s and $T_2 = 10$ s, each with either a fixed (green) or a self-consistently evolved equilibrium (red; $T_{\text{VMEC}} = T/20$). Every simulation starts with the vacuum reference magnetic equilibrium of W7-X discharge 20171206.036. In the high-frequency case (see figure 1), the rotational transform follows the ECCD modulation, whereas the total plasma current evolves on a slower timescale and exhibits no significant oscillations, resulting in a spectral peak only in the rotational transform. Owing to the relatively small plasma current, only minor differences are observed between the fixed and self-consistent equilibrium calculations in this regime.

For the low-frequency modulation (see figure 2), the plasma current also oscillates and reaches a periodically varying steady state around the calculated bootstrap current. While the fixed-equilibrium simulations exhibit a linear frequency response, the self-consistent calculations generate additional spectral components, most prominently the second harmonic of the drive frequency, through feedback between current diffusion and equilibrium evolution. These nonlinear features are particularly visible in the rotational transform spectrum, whereas they are barely visible in the plasma current spectrum. It should be noted that no sawtooth model is included in this toy simulation, allowing the rotational transform to exceed unity.

4 Validation against a W7-X discharge

In this section, the framework is validated against W7-X discharge 20171206.036. An overview of the temporal evolution of the main plasma parameters is shown in figure 3. Three ECRH beams were used for plasma

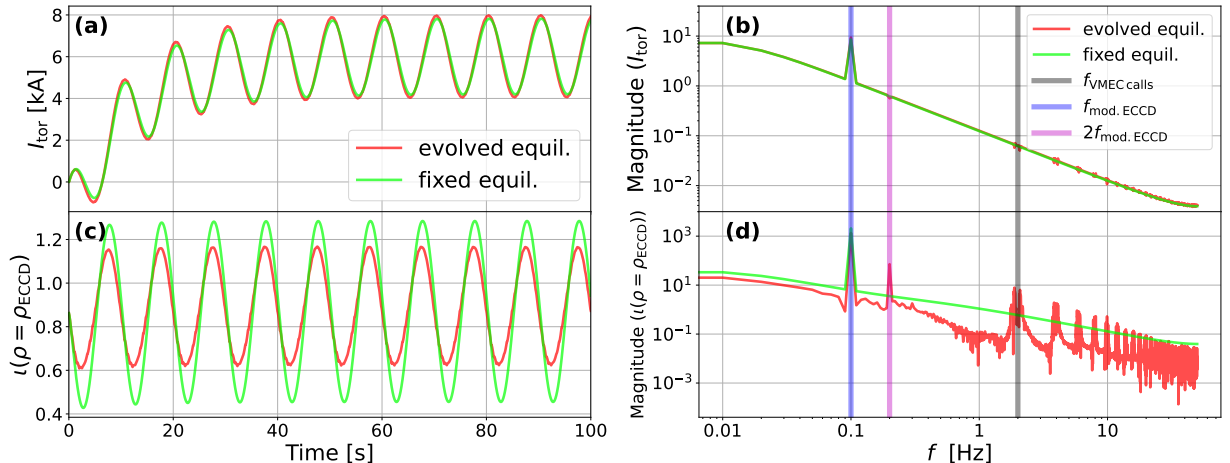


Figure 2: Low frequency case: (a)/(b) and (c)/(d): Evolution/Frequency spectrum of I_{tor} and $\iota(\rho = \rho_{\text{ECCD}})$. Comparison between fixed (green) and evolved equilibrium (red). ECCD modulation frequency (blue), 2nd harmonic frequency (magenta), and VMEC call frequency (grey) are indicated as vertical lines.

heating, as shown in figure 3.a, two of which were injected obliquely and therefore contributed to current drive. During the discharge, the electron density and temperature varied in time (see figures 3.c and 3.d). These variations have a significant impact on the ECCD efficiency, which scales approximately with T_e/n_e [9] (see figure 3.e). In addition, changes in the effective charge over the course of the discharge, see figure 3.f, further influence the ECCD efficiency.

In [4], the evolution of the toroidal plasma current was simulated using experimental n_e and T_e profiles taken from the time intervals indicated in figures 3.c and 3.d. Between these intervals, the profiles were interpolated in time. After 19.4s, the kinetic profiles were assumed to remain constant, which is justified up to approximately 23s, as indicated by the grey vertical line in figure 3. ECCD profiles were calculated for each time interval marked in figure 3.e using TRAVIS. The Z_{eff} profiles required for the TRAVIS calculations were also obtained from experimental data. The parallel conductivity was computed using the expression from [10], although it was originally derived for axisymmetric systems. The bootstrap current was prescribed as a time-independent parabolic profile with a total current of 2.5 kA. In that study, the vacuum reference equilibrium of discharge 20171206.036 was used as a fixed equilibrium. The corresponding simulated plasma current is shown in green in figure 3.g.

Using the recent developments in ASTRA, the simulation of discharge 20171206.036 was repeated with an evolving magnetic equilibrium, starting from the vacuum reference equilibrium of the discharge. In contrast to the previous simulation, both σ_{\parallel} and the bootstrap current were calculated self-consistently during the run using the DKES coupling. Furthermore, a coupling to TRAVIS was established in order to update the current drive density every 0.1s throughout the simulation. The experimental n_e , T_e , and Z_{eff} profiles were retained as input. The resulting current evolution is shown in red in figure 3.g.

The updated framework, in which the magnetic equilibrium, bootstrap current, and parallel conductivity are evolved self-consistently through the coupling to VMEC and DKES, reproduces the experimentally measured toroidal current evolution, shown in grey in figure 3.g. The remaining deviations can be attributed to uncertainties in the experimental n_e , T_e , and Z_{eff} profiles, which directly affect the ECCD, conductivity, and bootstrap current calculation. The previous fixed-equilibrium simulation also showed good agreement. However, it relied on a tokamak-based conductivity model, a prescribed parabolic bootstrap current profile, and a fixed magnetic equilibrium. Although only small differences are observed for this discharge, the updated framework is expected to be more generally applicable to stellarator plasmas.

5 Conclusions and Outlook

In the presented work, current diffusion in stellarator geometry was investigated in ASTRA using a generalised poloidal flux diffusion equation with self-consistent evolution of the magnetic equilibrium, bootstrap current, and parallel electrical conductivity. A proof-of-concept study with modulated ECCD showed that the rotational transform follows high-frequency modulation directly, while the total toroidal current evolves on a slower timescale. For low-frequency modulation, the plasma current oscillates around the bootstrap current level. With self-consistent equilibrium evolution, additional nonlinear spectral components arise from feedback between current diffusion and the magnetic geometry. Validation against W7-X discharge

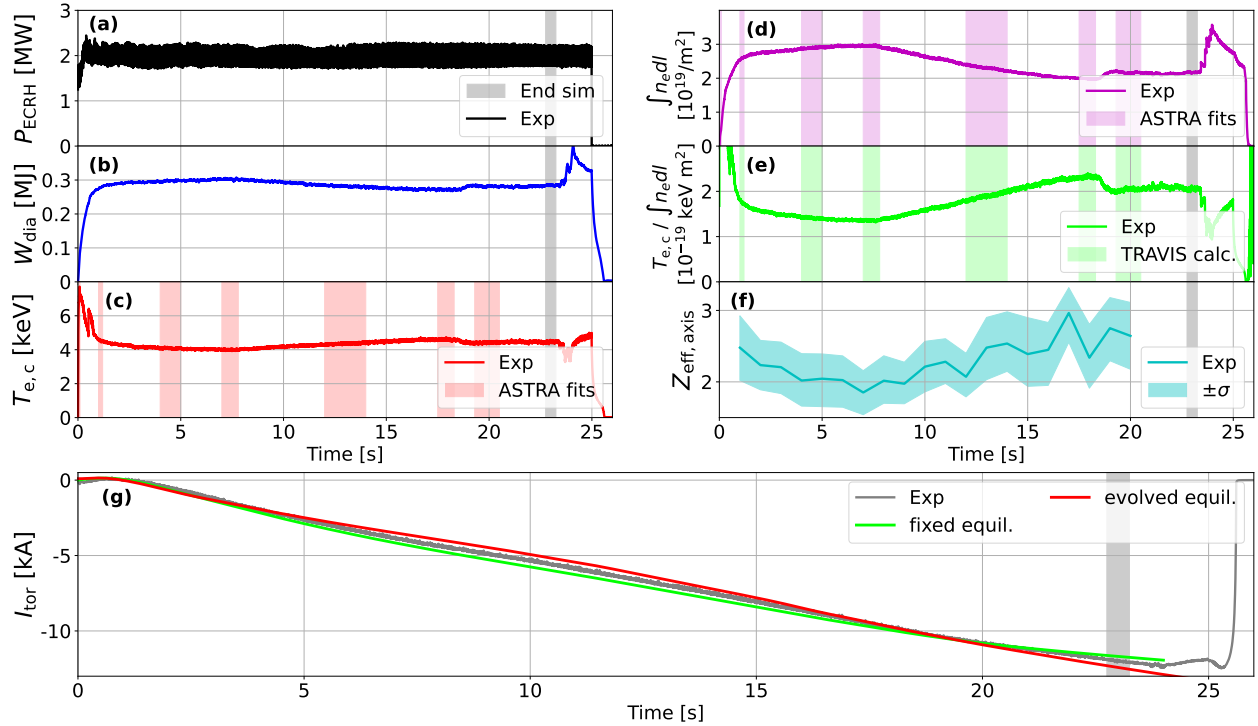


Figure 3: Evolution of plasma parameters during W7-X discharge 20171206.036. (g): Evolution of I_{tor} in simulation with evolved equilibrium (red) compared to simulation with fixed equilibrium (green) and experiment (grey).

20171206.036 showed that the measured toroidal current evolution is reproduced, with remaining deviations plausibly linked to uncertainties in the experimental n_e , T_e , and Z_{eff} profiles.

Future work will address the coupling of additional physics models, including neutral beam heating, turbulent transport, and scrape-off-layer particle and power exhaust, to enable predictive simulations of density and temperature profile evolution. The newly implemented self-consistent equilibrium evolution will be particularly important for future simulations of discharges with significant changes in plasma β , where the magnetic configuration may be strongly affected [11].

Acknowledgements

This work was funded by the Federal Ministry of Research, Technology and Space in Germany under project FPP-MC (13F1001A). This work has also been carried out within the framework of the EUROfusion Consortium, funded by the European Union via the Euratom Research and Training Programme (Grant Agreement No. 101052200 — EUROfusion). Views and opinions expressed are, however, those of the author(s) only and do not necessarily reflect those of the Federal Ministry of Research, Technology and Space in Germany, the European Union, or the European Commission. Neither the Federal Ministry of Research, Technology and Space in Germany, the European Union, nor the European Commission can be held responsible for them.

References

- [1] G. V. Pereverzev and P. N. Yushmanov 2002 ASTRA. Automated System for Transport Analysis in a Tokamak. *IPP Report* Nr. 5-98
- [2] G. Tardini *et al* 2026 *Plasma Phys. Control. Fusion* **68** 065024
- [3] P. David *et al* 2025 *Open Plasma Sci.* **1** 3
- [4] F. Solfronk *et al* 2026 *Plasma Phys. Control. Fusion* **68** 045012
- [5] S. P. Hirshman and J. C. Whitson 1983 *Phys. Fluids* **26** 3553
- [6] E. Fable *et al* 2026 submitted to *Plasma Phys. Control. Fusion*
- [7] E. Buglione-Ceresa 2025 *Master's thesis*
- [8] N. B. Marushchenko *et al* 2014 *Comput. Phys. Commun.* **185** 165–76
- [9] T. C. Luce *et al* 1999 *Phys. Rev. Lett.* **83** 4550
- [10] O. Sauter *et al* 1999 *Phys. Plasmas* **6** 2834–2839
- [11] P. Helander *et al* 2012 *Plasma Phys. Control. Fusion* **54** 124009